Investigating the Remyelination Effects of Myricetin After Demyelination Caused by Experimental Pressure Applied to the Optic Chiasm in Rats

Eren Yilmaz , Ihsan Anik * , Sibel Kokturk , Atakan Emengen , Ayse Uzuner , Ayse Karson , Sibel Balci , Aykut Gokbel , Melih Caklili , Burak Cabuk , Savas Ceylan

Posted Date: 29 July 2025

doi: 10.20944/preprints202507.2316.v1

Keywords: Demyelination; Remyelination; Myricetin; Experimental; Optic Chiasm

 doi:10.20944/preprints202507.2316.v1

Article

Investigating the Remyelination Effects of Myricetin After Demyelination Caused by Experimental Pressure Applied to the Optic Chiasm in Rats

Short Title: Stereotactic Optic Compression and Myricetin

Eren Yilmaz [1], Ihsan Anik *[2], Sibel Kokturk [3], Atakan Emengen [4], Ayse Uzuner [5], Ayse Karson [6], Sibel Balci [7], Aykut Gökbel [1], Melih Caklili [2], Burak Cabuk [2] and Savas Ceylan [4]

[1] Department of Neurosurgery, Istinye University, Istanbul, Turkey
[2] Department of Neurosurgery, Kocaeli University School of Medicine, Pituitary Research Center, Kocaeli, Turkey
[3] Istanbul University, Faculty of Medicine, Department of Histology and Embryology, Istanbul, Turkey
[4] Department of Neurosurgery, Bahcesehir Universty School of Medicine, Istanbul, Turkey
[5] Department of Neurosurgery, Afsin State Hospital, Kahramanmaras, Turkey
[6] Kocaeli University, Faculty of Medicine, Department of Physiology, Kocaeli, Turkey
[7] Department of Biostatistics and Medical Informatics, Kocaeli University, Kocaeli, Turkey
* Correspondence: drianik@yahoo.com; Telephone : +905332476735; ORCID 0000-0003-2567-7969

Abstract

Background/Objectives: The aim of this study was to induce demyelination in rats by placing a balloon catheter applying pressure under the optic chiasm using a stereotaxic device, and subsequently examine the effects of myricetin, a neuroprotective agent, on the demyelination/remyelination processes using electron microscopy. **Methods:** A total of 40 adult male Wistar albino rats were used to establish an experimental model of optic chiasm compression via stereotaxic placement of a neuroballoon catheter. Animals were divided into four groups: control, demyelination, remyelination, and myricetin treatment. After catheter-induced compression, demyelination and remyelination processes were evaluated. Myricetin was administered intraperitoneally in the treatment group. Optic chiasm tissues were harvested and analyzed histopathological and ultrastructurally using electron and light microscopy. Statistical analyses were performed using chi-square tests, with $p<0.05$ considered significant. **Results:** When the demyelination and remyelination groups were compared with the control group, severe degeneration accompanied by Wallerian degeneration was observed, along with demyelination in axons, vacuolization in oligodendrocytes, and dark axonal degeneration. Compared to the other groups, the myricetin group showed a reduction in dark degeneration, axonal demyelination, and degeneration. **Conclusions:** This study represents another example of experimental models of demyelination resulting from optic chiasm compression, which are rare in the literature. Myricetin has been shown to have positive effects on remyelination and may guide subsequent studies. Furthermore, this experimental model may allow the investigation of the demyelination and remyelination effects of different agents in the optic chiasm.

Keywords: Demyelination; Remyelination; Myricetin; Experimental; Optic Chiasm

1. Introduction

The lack of regenerative and axonal growth capacity in the central nervous system has led to research aimed at reversing this process [1-4]. The optic nerve tissue, being a component of the central nervous system, can be easily examined and is relatively easily accessible, due to which it ranks

 doi:10.20944/preprints202507.2316.v1

topmost in studies on degeneration and regeneration processes in the central nervous system[5-9]. Consequently, researchers have attempted to clarify issues such as the inhibitory effects of myelin, glial scar, neuroinflammation, and apoptosis by generating experimental models that cause chemical, electrical, and mechanical damage to the optic nerve and retinal ganglion cells for investigating regenerative failure in the central nervous system[10-15].

Visual field defects are a vital clinical finding that occur with the growth of lesions located in the sellar region toward the suprasellar area. The disruption of signal transmission in chiasmatic axons under pressure is an indicator of axonal damage[16,17]. The improvement in the visual field after surgical decompression varies according to the remyelination processes in the optic nerve. In two previous studies conducted in our center, demyelination occurring after compression in the optic chiasm and remyelination occurring after surgical decompression in patients were demonstrated radiologically by diffusion tensor imaging (DTI), a specialized form of magnetic resonance imaging (MRI) [18,19].

Although mechanical compression, toxin-based, chemical, and virus-mediated animal models are commonly used to investigate demyelination and remyelination processes in the optic nerve, experimental animal models that specifically mimic mechanical compression of the optic chiasm remain limited. To address this gap, our group previously developed a stereotactic balloon compression model in rats to simulate mechanical compression of the optic chiasm[20]. Building on that prior work, we designed the current study to investigate the effects of myricetin—a natural flavonoid known to cross the blood–brain barrier and exhibit antioxidant, anti-inflammatory, and neuroprotective properties—on remyelination in the optic chiasm. The aim of this study was to first induce demyelination in the rat optic chiasm by applying inferior mechanical compression, and then to evaluate the potential effects of myricetin on remyelination processes after the removal of compression.

2. Material and Methods

This study, which included 40 rats using the stereotaxic technique, was conducted at the Kocaeli University Experimental Medicine and Research Unit. Approval for conducting this study was obtained from the Kocaeli University Local Ethics Committee for Animal Experiments with the project number KOU HADYEK 7/1-2022. All experiments were performed in accordance with relevant international guidelines and regulations on the use of experimental animals. Additionally, the authors confirm that the study was conducted in accordance with ARRIVE guidelines. Histological examination was conducted by the Department of Histology and Embryology at Istanbul University Faculty of Medicine.

2.1. Animals

Adult male Wistar albino rats weighing an average of 280–300 g and aged 16–20 weeks were used in this study. We chose male rats to reduce variability in biological and hormonal fluctuations related to the estrous cycle that could affect neuroinflammation and demyelination. The rats were housed in an environment with controlled room temperature (23℃ ± 2℃) and day–night cycle (12 hours light / 12 hours dark), with four animals kept in a single cage. The animals were fed ad libitum. The surgical procedure was performed in the same operating room under the same conditions for each animal during the same time period of the day, and the animals were followed up in individual cages after the procedure. Throughout the experimental period, all procedures were performed according to the procedures specified in international regulations on the use of animals used for experimental or other scientific purposes.

2.2. Myricetin

Myricetin is a natural flavonoid commonly found in several natural plants and has multiple biological functions, showing promising results in research[21]. Modern pharmacological studies have demonstrated that myricetin exhibits anti-inflammatory[22], antitumor[23,24], antibacterial[25], antiviral[26], and protective activities against cardiovascular[27]/hepatic damage[28] in addition to

 doi:10.20944/preprints202507.2316.v1

neuroprotective effects[21,29-32], providing protection against neurological damage. The ability of flavonoids to cross the blood–brain barrier suggests that it can exert a direct effect on the brain.

Inhibition of transferrin receptor-1 expression, activation of antioxidant enzymes, and reduction of lipid peroxidation can decrease brain iron ion levels, thereby reversing cognitive dysfunction in the brain[21,33]. In prolonged stress, an increase in Adrenocorticotropic hormone (ACTH) and a decrease in brain-derived neurotrophic factor (BDNF) in the hippocampus are observed. Myricetin reduces ACTH levels and increases BDNF expression, improving stress-induced memory impairment[30]. It positively contributes to the differentiation of glial cells and the maturation of hippocampal dentate neurons[34]. By preventing nitric oxide diffusion and promoting hippocampal neurogenesis, it exhibits antidepressant-like and atypical antipsychotic-like effects[21,34]. Tyrosine hydroxylase (TH) enhances mTORC1 activation and inhibits TNF-α expression, thereby protecting dopaminergic neurons and ameliorating 6-hydroxydopamine (6-OHDA)-induced dopaminergic neuron degeneration[35]. Oxidative damage to mitochondria leads to oxidative stress by increasing cerebral ischemic/reperfusion injury. The Nrf2-ARE pathway is a defense mechanism against oxidative stress. Myricetin activates Nrf2, upregulates ARE, thereby improving mitochondrial function and protecting against cerebral ischemia[36]. An experimental study on mice has shown that it alleviates demyelination[33].

2.3. Stereotaxic Surgical Method

Each rat was deeply anesthetized in the operating room with an intraperitoneal injection of ketamine (90 mg/kg) and xylazine (10 mg/kg). The depth of anesthesia was evaluated using pain tests. The rats were then fixed in a stereotaxic apparatus (Stoelting stereotaxic device) in a flat-skull position, with the anterior upper incisors parallel to the ground. After applying a local anesthetic under the skin, an average 15-mm linear skin incision was made along the midline from between both eyeballs passing over the bregma (the intersection of the sagittal and coronal sutures). After retracting the periosteum to both sides, the bregma was exposed. Using a stereotaxic apparatus, a burr hole was opened on the midline, 6.2 mm anterior to the bregma (where the two optic nerves enter the optic canal according to the atlas of Paxinos & Watson) [37], using a high-speed drill. Then, an incision was made on the sagittal sinus in the midline, the dura was opened, and bleeding from the sagittal sinus was controlled with the help of a hemostatic agent. After checking the neuroballoon catheter (2 French), it was advanced perpendicularly through the burr hole into the skull. When the catheter reached the base of the skull, it was directed posteriorly. In cadaver studies, the distance between the burr hole and optic chiasm was measured as 7 mm[20]. When it reached the base of the skull, the neuroballoon catheter was advanced 7 mm posteriorly along the midline, passing between the two optic nerves. The air inside the neuroballoon catheter was removed, and it was inflated with 0.5 cc of saline to create mechanical compression on the optic chiasm from below. The catheter was fixed by tying it immediately after the burr hole and soldering it with a heat-generating soldering device to prevent fluid leakage. Then, the neuroballoon catheter was fixed subcutaneously with acrylic, and the skin incision was closed with sutures (Figure 1 and Video 1).

 doi:10.20944/preprints202507.2316.v1

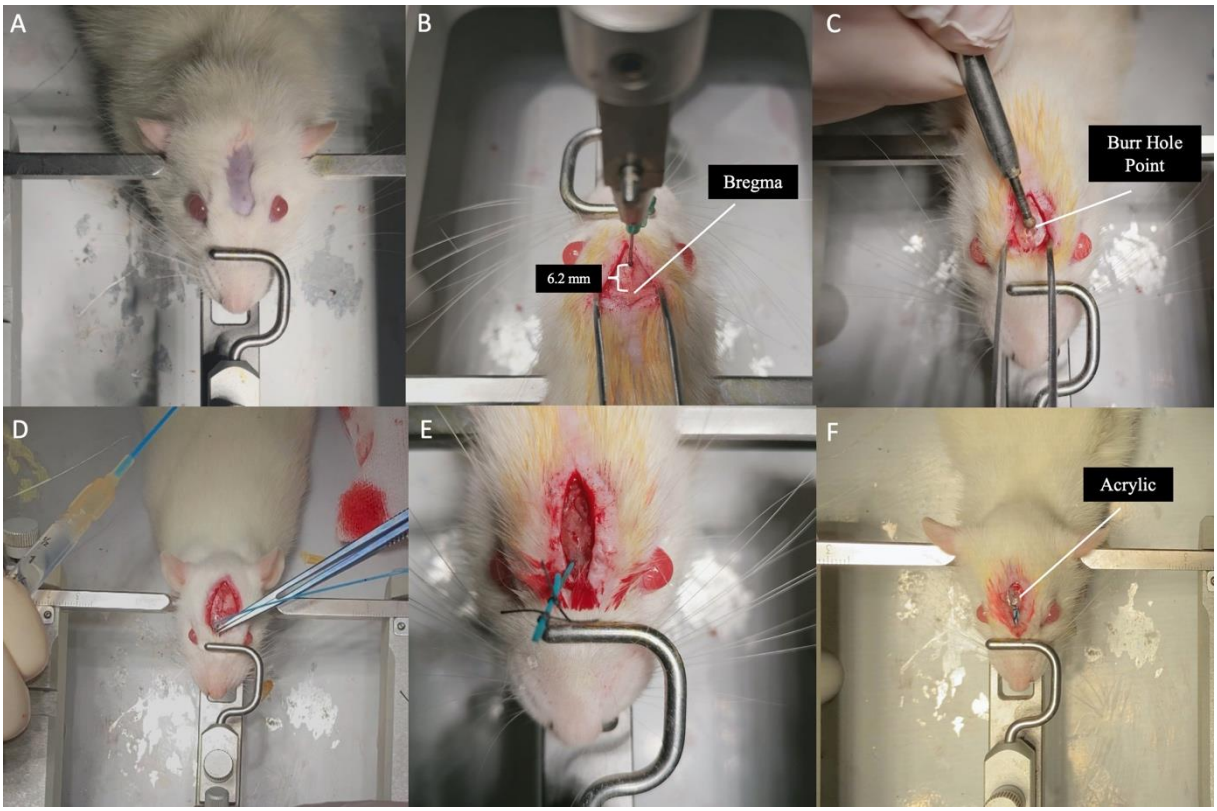

Figure 1. A: Placing the rat in the stereotaxy device. **B:** Revealing the Bregma point after skin incision and determining the Burr-hole point 6.2 mm anterior to the Bregma point. **C:** Burr-hole opening with a high-speed drill. **D:** Advancing the 2F catheter vertically from the Burr-hole to the skull base and then advancing it 7 mm posteriorly and inflating the catheter with saline. **E:** After the catheter is placed, the extracranial part is tied with non-absorbable thread and cut with a heat-generating soldering device to prevent saline leakage. **F:** Fixing the catheter to the cranium with acrylic to prevent catheter displacement before skin suturing.

2.4. Experimental Model and Grouping of Animals

Demyelination occurs 2 days after optic nerve compression in rats, and complete demyelination occurs in the axons after 7-10 days, and it has been reported that remyelination is observed within 7-14 days[38,39]. The animals were divided into four groups: Group 1, Group 2, Group 3, and Group 4, with 10 rats in each group (Table 1).

In Group 1, the optic chiasm was removed and histologically examined under an electron microscope after decapitating the rats under deep anesthesia without any surgical procedure. Groups 2,3,4 were subjected to the stereotaxic surgical procedure, with the neuroballoon catheter placed inferior to the optic chiasm. In Group 2(demyelination group), the rats were decapitated under deep anesthesia(ketamine (90 mg/kg) and xylazine (10 mg/kg)) on the 10th day after catheter placement; this group served as the demyelination group and helped control the position of the catheter (Figure 2). After decapitating the rats in Group 2, the saline inside the catheter was emptied, and the catheter was removed. The catheters of rats in Groups 3 and 4 were removed on the 10th day after placement, after emptying the saline inside under general anesthesia. In Group 3(remyelination group), the rats were followed up in individual cages after catheter removal and decapitated under deep anesthesia(ketamine (90 mg/kg) and xylazine (10 mg/kg)) on the 10th day. In Group 4 (myricetin group), myricetin was injected intraperitoneally at a dose of 25 mg/kg immediately after removing the catheter, followed by 10 days of observation in individual cages, based on previous reports indicating that remyelination begins within 7–14 days following optic nerve decompression[20,38]. On the 10th day, the rats were decapitated under deep anesthesia (Figure 3). After all decapitations, the optic chiasm was removed by anatomical dissection and placed in glutaraldehyde solution at +4°C for examination under an electron microscope.

Table 1. Study Groups and Number of Samples.

 doi:10.20944/preprints202507.2316.v1

	Groups	Anima l	Live Animal	Number of Glutaraldehyd e Samples
Group 1	Control	10	0	10
Group 2	Demyelination group following compression	10	9	9
Group 3	Remyelination group following compression	10	8	8
Group 4	Myricetin applied group following compression	10	8	8

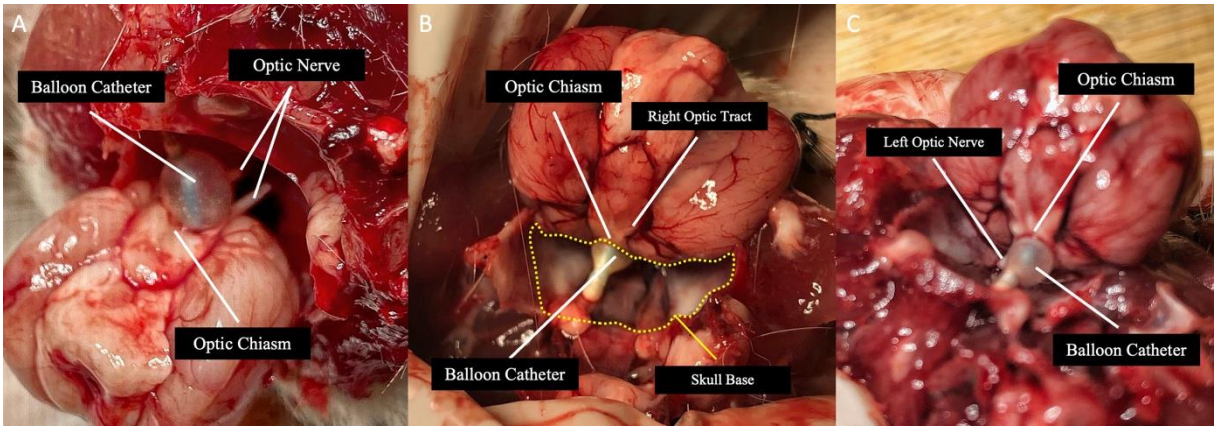

Figure 2. A,B,C: The appearance of balloon catheter, optic chiasm, optic nerves, and optic tract after decapitation of three different rats within Group 2, where demyelination was evaluated.

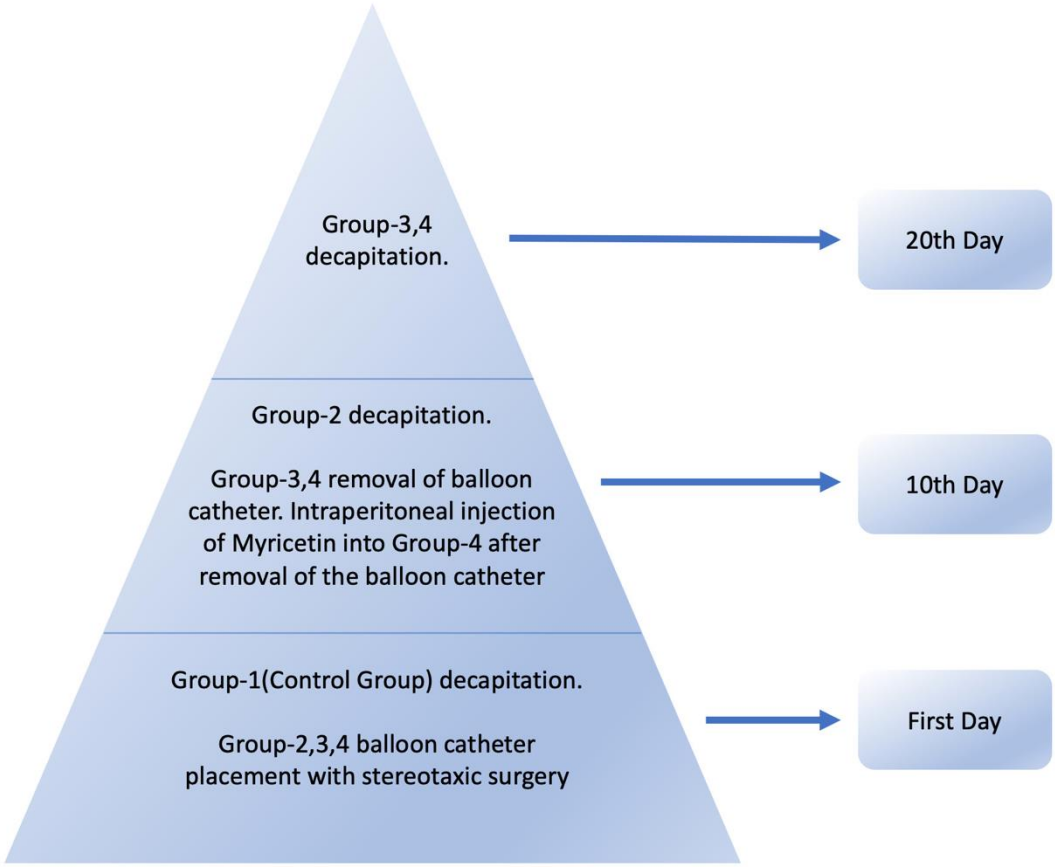

Figure 3. Experimental Process.

 doi:10.20944/preprints202507.2316.v1

2.5. Ultrastructural and Histological Evaluation

Tissues obtained from the optic chiasms of rats were observed under an electron microscope to examine their ultrastructural features. For electron microscopy, the tissues were fixed in a 2.5% glutaraldehyde solution at +4°C, washed in phosphate buffer at +4°C for 10 minutes, and then placed in 1% osmium acid at +4°C for 1 hour, followed by another washing in phosphate buffer at +4°C for 10 minutes. For contrast, they were placed in 1% uranyl acetate at +4°C for 30 min and then washed again in phosphate buffer at +4°C for 10 min. Then, the optic chiasms were placed in 30% and 50% alcohol for 10 min and in 70% alcohol at +4°C overnight. Next, they were passed through 90% and 100% alcohol at room temperature for 10 min each, followed by two 10-min washes in propylene oxide solution. The optic chiasms were then placed in propylene oxide–epon mixtures at ratios of 1:1 and 1:3 and in pure epon at room temperature for 1 h. Finally, the optic chiasms were embedded in epon capsules and placed at 60°C in an oven for approximately 18 h until polymerization. Sections measuring approximately 60 nanometers in thickness were cut from the epon blocks using a Leica EM UC7 ultramicrotome and placed on grids. The grids containing the sections were contrasted with uranyl acetate and lead nitrate solutions and examined and photographed using a Jeol JEM 1011 transmission electron microscope.

The semi-thin optic chiasms cross-sections of groups (n=5) stained with the methylene blue stain. The images captured with 100x magnification of Zeiss Primo Star 3 light microscope. The percent of myelin areas were analyzed from the randomly selected 3 images using NIH ImageJ software. The results evaluate the one-way analysis of variance (ANOVA) and Tukey multiple comparison tests by KaleidaGraph 4.0 software. p values < 0.05 were considered significant.

The results of morphometric evaluation of cells and myelinated fibers were classified into three grades according to the severity and extent of destruction, as follows: I, slight pathological changes, including myelin lamina rarefaction and focal demyelination or vacuolization, with the axon being less affected; II, moderate pathological changes, including myelin lamina reticulation, focal demyelination, vacuolization, and axonal changes, such as increased electron density, lipofuscin deposition, and glycogen granules; and III, severe pathological changes, including marked myelin damage or disruption, accompanied by axonal degeneration and loss[40].

2.6. Statistical Analysis

All statistical analyses were performed using IBM SPSS for Windows version 29.0 (IBM Corp., Armonk, NY, USA) software. Categorical variables were summarized as counts and percentages. Associations between categorical variables were examined by Chi-square test. A p-value of <0.05 was considered statistically significant.

Due to ethical constraints, we used the maximum number of animals permitted by the Kocaeli University Local Ethics Committee (n=8-10 per group). As the sample size was pre-determined by the ethics approval, a priori power analysis could not be performed. However, to evaluate the statistical power of our findings, we conducted a post-hoc power analysis based on the obtained results. This analysis was carried out using PASS 11 software, with the significance level (α) set at 0.05. The calculated effect size was 0.74, and the statistical power of the study was determined to be 92%.

3. Results

One of the rats in Groups 2 and 3 and two rats in Group 4 died on the 1st day after the first surgical procedure. One of the rats in Group-3 died on the 1st day after the removal of the balloon catheter. The fact that all observed mortalities occurred within the first 24 hours after surgery strongly suggests that they were related to procedural complications rather than inadequate animal care or welfare. It is most likely that these early postoperative deaths resulted either from re-bleeding of the sagittal sinus—despite intraoperative hemostasis—or from acute intracranial pressure elevation leading to herniation, caused by the inflation of the neuroballoon catheter. The absence of any deaths after the first postoperative day supports this situation. The number of glutaraldehyde-fixed samples was 10 in Group 1, 9 in Group 2, and 8 each in Groups 3 and 4.

 doi:10.20944/preprints202507.2316.v1

In Group 1, the oligodendrocyte nucleus contained a patchy pattern of heterochromatin and euchromatin and was surrounded by a narrow rim of pale cytoplasm. Morphologically normal ribosomes, mitochondria, and cisterns of endoplasmic reticulum were abundant in the cytoplasm of oligodendrocytes. The axons were surrounded by well-compacted myelin sheaths. The myelin sheaths contained smooth and tightly attached myelin lamellae (Figure 4).

Seven out of 9 rats (77.8%) in the demyelination group (Group 2) showed severe pathological changes in which oligodendrocytes showed numerous heterochromatic nuclei and chromatin condensation. The cytoplasm of swollen oligodendrocytes appeared dense and uniformly granular due to scattered ribosomes. The cytoplasm also contained dilated mitochondria and cisterns of endoplasmic reticulum. The swollen axons appeared pale and enlarged with axolemmal expansion characterizing watery degeneration (axonal swelling). Several axons contained multilayered whorled masses, myelin debris, and blebs, which appeared to be arising from the inner layers of myelin. In some axons, their axoplasm was filled with a granular and dark material, described as dark degeneration (hyperdense axoplasm). The dark axons exhibited myelin changes such as lamellar separation and widening. Severe decompaction of lamellae made the myelin appear wave-like. Demyelinating changes such as loss of myelin (demyelination), myelin breakdown, and detached and vacuolated lamellae were frequently detected (Figure 5 A,B).

6 of 8 rats (75%) in the remyelination group (Group 3) showed severe pathological changes. In the remyelination group, the oligodendrocytes exhibited mitochondrial swelling, dilated cisterns of endoplasmic reticulum, and heterochromatic changes in nuclear morphology. The remyelination group also showed watery degeneration with vacuoles, dark degeneration, demyelination, separation of myelin lamellae, and whorl-like multilaminated myelin-like bodies in severely damaged axons (Figure 5 C,D).

In the myricetin group (Group 4), 7 out of 8 rats (87.5%) showed slight pathological changes with a decrease in the number of vacuoles in the cytoplasm of axons and oligodendrocytes. Compared with the other groups, these 7 rats showed a decrease in dark degeneration and demyelination and axon degeneration (Figure 6).

In the statistical analysis performed in terms of histopathological changes of the groups, the slight pathological change observed at a rate of 87.5% in the myricetin injected group (Group 4) was statistically significant compared to Groups 2 and 3 *(p:0.001)*. Similarly, the severe pathological changes observed in Group 2 and Group 3 were statistically significant when compared to Group 4 *(p:0.002)*.(Table 2).

In experimental nerve repair studies, axon and myelin sheath measurements are critical to determine to the myelin loss and the regenerating nerves. Semi-thin sections were stained with methylene blue and analyzed by light microscopy. The percent of myelin area measurements of methylene blue-stained optic chiasm revealed whether there was optic chiasm myelin loss. In the control group (group 1), observed numerous oligodendrocytes with pale nuclei and irregular cytoplasmic shape with normal features. In the control group, *myelin sheaths were dense and smooth in appearance*, and vacuoles were absent (Figure 7A, Figure 8 and $p < 0.001$).

In the demyelination group (group-2), large and numerous vacuoles and patches of empty space without myelin shealth were observed. Ultrastructural features also showed the loss of axonal profiles in the demyelination group. In the demyelination group, observed a few oligodendrocytes. The optic chiasm was characterized by the severe loss of axonal profiles in the demyelination group compared to the control group and other groups (Figure 7B, Figure 8 and $p < 0.001$). Numerous and small sizes vacuoles and patches of empty space without myelin shealth were detected in the remyelination group. In the remyelination group, observed a few oligodendrocytes. In the remyelination group (group-3), observed irregular myelination and thinner myelin sheaths compared to the control group and other (Figure 7C, Figure 8 and $p < 0.001$). In the myricetin group (group-4), observed irregular myelination and thinner myelin sheaths compared to the control group ($p < 0.001$). However, the myelination was increased in the myricetin group compared to the demyelination and remyelination groups (Figure 7D, Figure 8 and $p < 0.001$). A few small vacuoles were appeared in the myricetin group.

 doi:10.20944/preprints202507.2316.v1

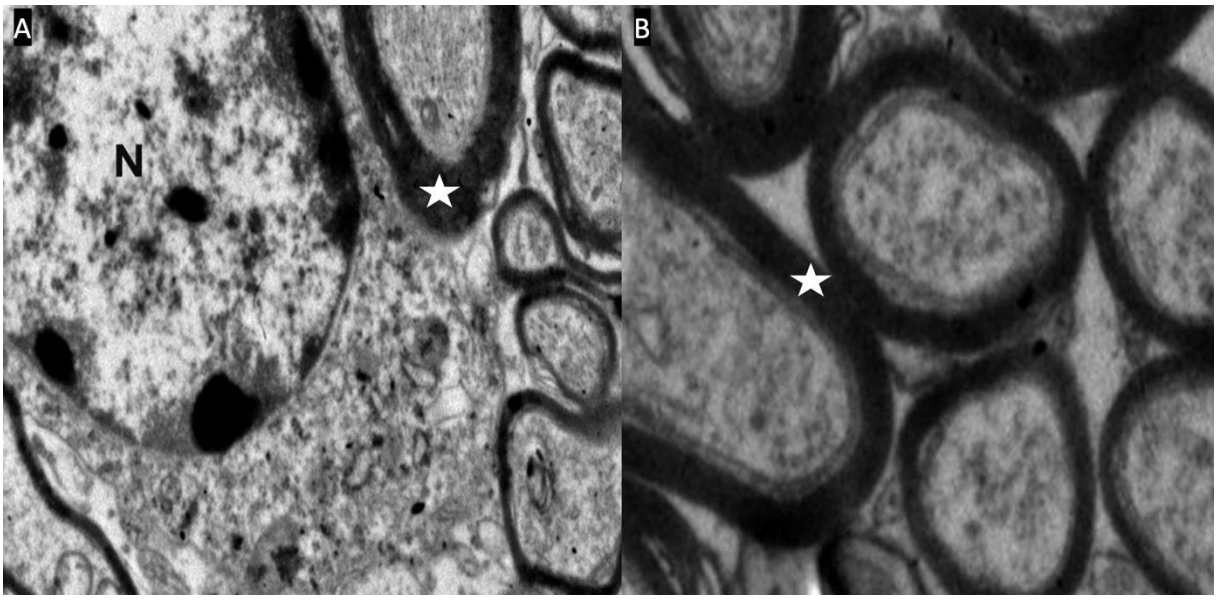

Figure 4. A,B: Optic chiasm electron microscope photographs of the control group (Group-1). The nucleus (N) of the oligodendrocyte and the myelin sheaths (white star) surrounding the axons are seen.

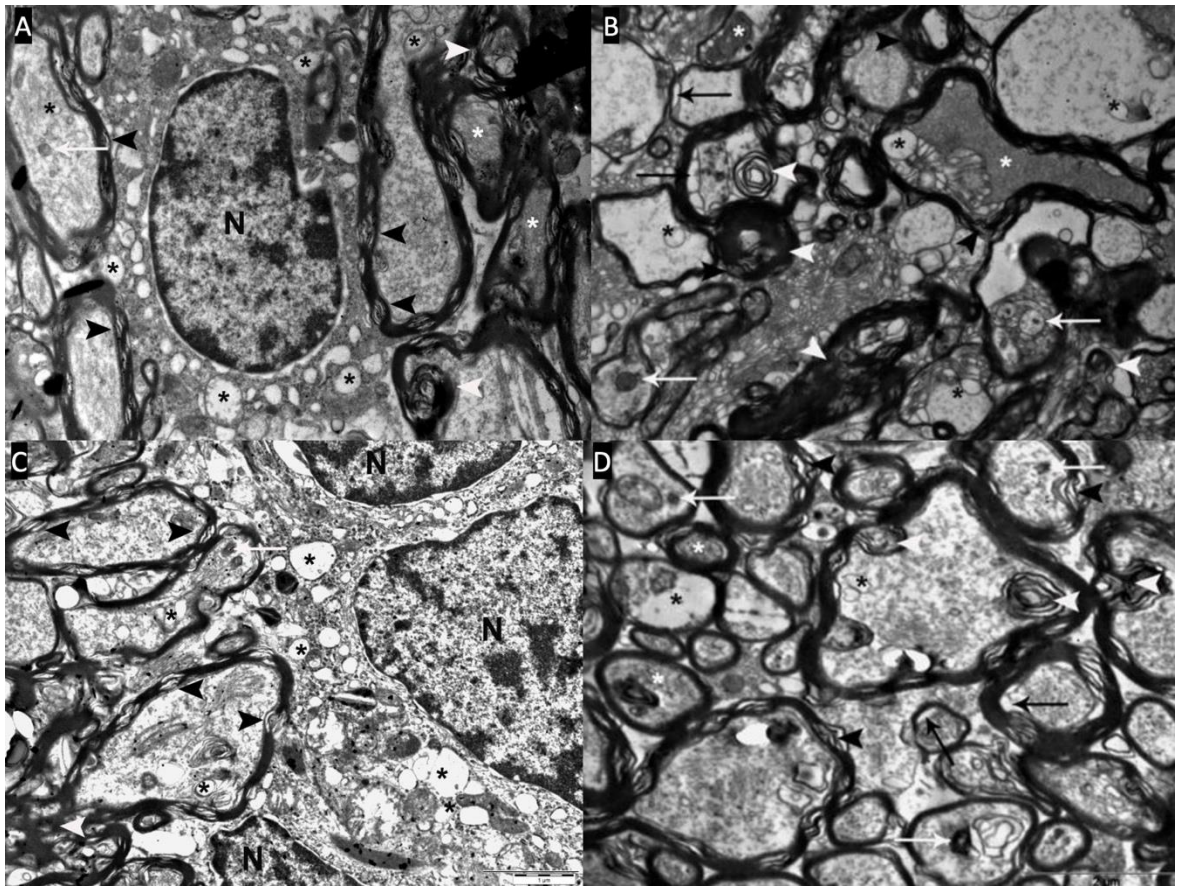

Figure 5. A,B: Severe pathological changes(Type-III) are observed in the optic chiasm electron microscopy of the demyelination group (Group-2). Myelin bleb and debris (white arrowhead), axolemma-myelin separation (black arrow), myelin sheath loss and separation (black arrowhead), vacuoles (black asterisk) and inclusions (white arrow) in axons and oligodendrocyte cytoplasm, dark axons (white asterisk) and oligodendrocyte nucleus (N). **C,D:** Severe pathological changes(Type-III) are observed in the optic chiasm electron microscopy of the remyelination group (Group-3). Myelin bleb and debris (white arrowhead), axolemma-myelin separation (black arrow), myelin sheath loss and separation (black arrowhead), vacuoles (black asterisk) and inclusions (white arrow) in the cytoplasm of axons, dark axons (white asterisk) and oligodendrocytes nucleus (N).

 doi:10.20944/preprints202507.2316.v1

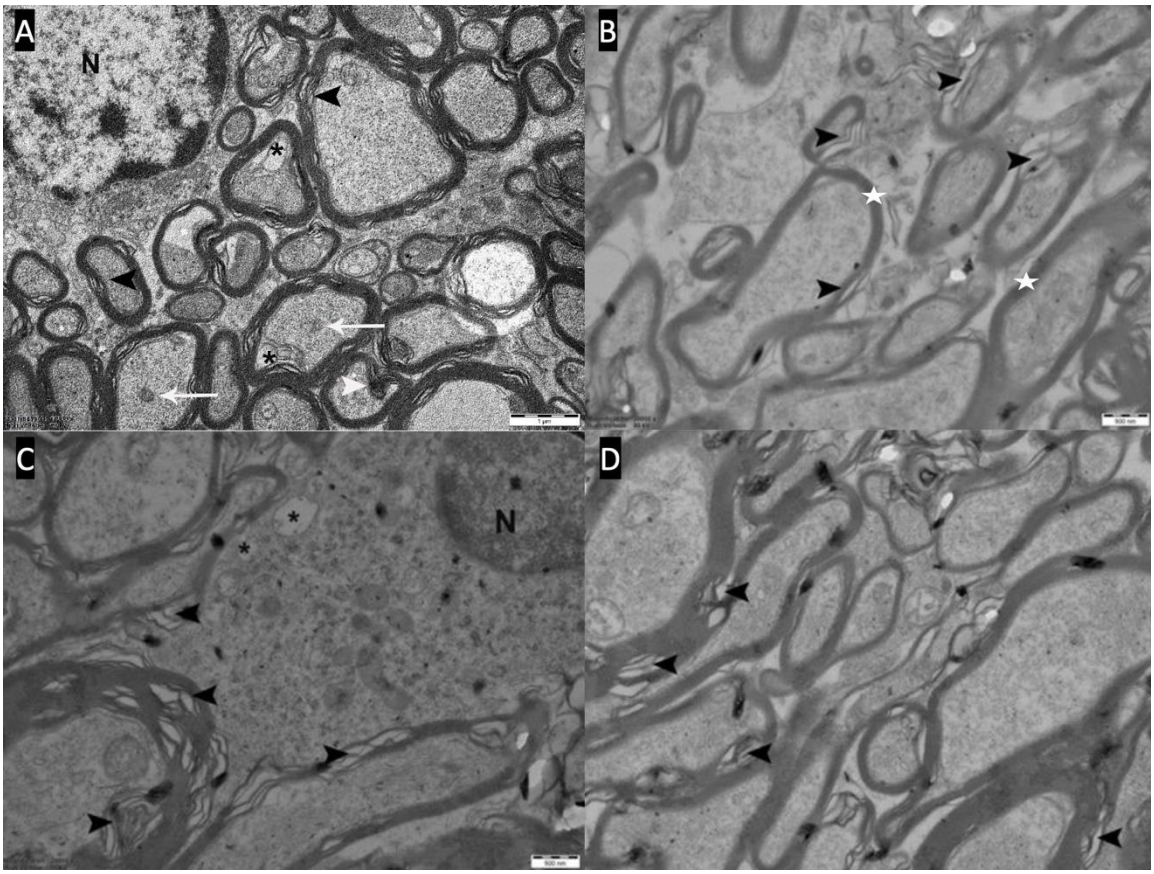

Figure 6. A,B,C,D: Slight pathological changes (Type-I) are observed in the optic chiasm electron microscopy of the myricetin group (Group-4). There is a decrease in myelin budding and degeneration (white arrowhead), a decrease in inclusions (white arrow) and vacuoles (black asterisk) in axons and oligodendrocyte cytoplasm. Myelin sheaths surrounding the axons (white star) and occasional myelin sheath loss (black arrowhead) are seen.

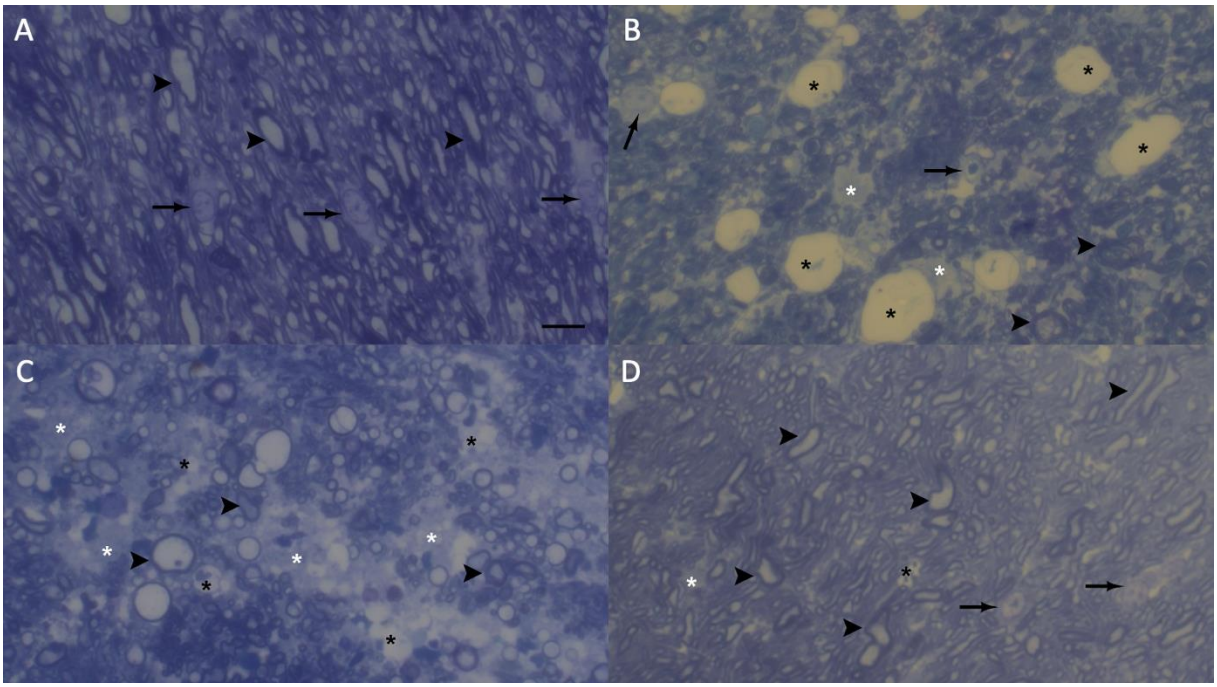

Figure 7. Representative electron microscopy semi-thin images taken from methylene blue-stained the optic chiasm sections of the groups. Control group (A), demyelination group (B) remyelination group (C) and myricetin group (D). Myelin shealths are shown as darkly stained circles. The vacuols and empty spaces are shown in light color. The arrow, oligodendrocyte; black asterisk, vacuoles; white asterisk, empty spaces and arrowhead, myelin shealth. Methylene blue stain and scale bar represents 10 μm.

 doi:10.20944/preprints202507.2316.v1

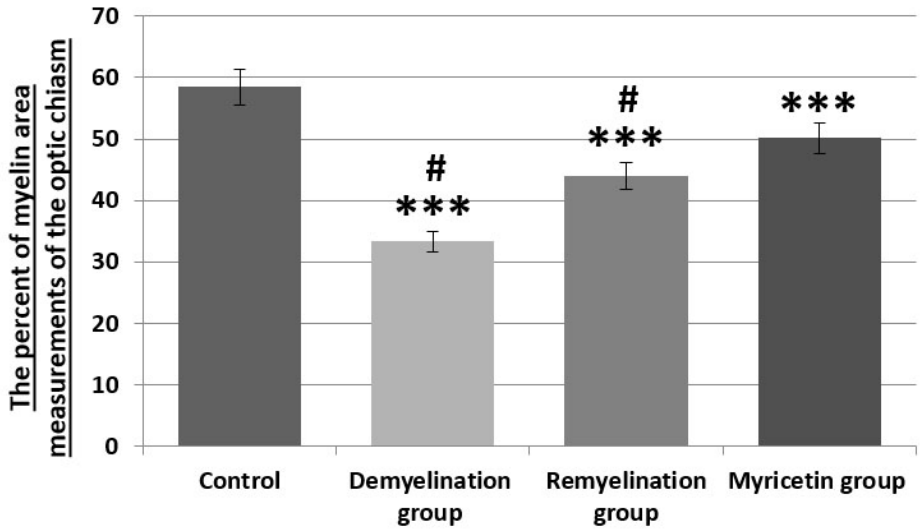

Figure 8. The percent of myelin area measurements of the optic chiasm with NIH ImageJ. Quantification of axon loss in the groups. n =5 group; *** $p < 0.001$ and # $p < 0.001$ compared to the control and myricetin group.

Table 2. Histopathological results and statistical evaluation of the groups.

	G1 (n=10)	G2 (n=9)	G3 (n=8)	G4 (n=8)	p value*
Degeneration Violence, n(%)					
None	10 (100)	0	0	0	-
Slight Pathological Changes	0	1 (11.1)[a]	1 (12.5)[a]	7 (87.5)[b]	**0.001**
Moderate Pathological Changes	0	1 (11.1)	1 (12.5)	1 (12.5)	1.00
Severe Pathological Changes	0	7 (77.8)[a]	6 (75)[a]	0[b]	**0.002**

G1: Group 1, G2: Group 2, G3: Group 3, G4: Group 4. *Chi-square test was used. Different uppercase letters indicate statistically significant differences between Group 2, Group 3 and Group 4.

4. Discussion

Animal models are effective for exploring the mechanisms underlying demyelination and remyelination processes and have been the subject of several studies. There are experimental models established to induce demyelination in the central nervous system in animals, such as autoimmunity-induced, virus-induced, toxin-induced, or experimental models established to increase remyelination[13,14,41-47]. Nevertheless, there is limited research investigating these processes by applying external pressure to the neural tissue[48,49].

As our institution is a high-volume tertiary center for endoscopic endonasal surgical treatment of lesions located in the sellar/parasellar region, we planned an experimental study that will mimic the mechanical compression applied to the optic chiasm by lesions in this region. This experimental animal model was previously described in our clinic, wherein demyelination processes were investigated by applying different mechanical pressures inferior to the optic chiasm using a balloon catheter, and remyelination processes were examined after removing the mechanical pressure[20]. In the present study, unlike our previous study, we not only demonstrated the demyelination and degeneration processes occurring in the optic chiasm under the same pressure in rats but also ultrastructurally examined the effects of an exogenously injected substance (myricetin) on demyelination and remyelination. The results of electron microscopy revealed demyelination and degeneration in the optic chiasm with the balloon catheter, and myricetin administration reduced demyelination and increased remyelination. Therefore, this study has two major significances. First,

 doi:10.20944/preprints202507.2316.v1

it contributes to the limited number of experimental models in the literature that apply external pressure to the neural tissue in the central nervous system. Second, it paves the way for follow-up studies on the use of myricetin to reduce demyelination and increase remyelination after the surgical decompression of lesions in the sellar/parasellar region that cause demyelination and degeneration in the optic chiasm.

If remyelination processes are to be investigated, demyelination must first be induced in the neural tissue. One of the models that causes demyelination in the literature is experimental autoimmune encephalomyelitis, which is the most commonly used model for studying autoimmune encephalitis in the central nervous system[1]. This model is typically induced by immunization with myelin antigens such as myelin basic protein, proteolipid protein, or myelin-oligodendrocyte glycoprotein, by the transfer of antigen-sensitized T cells, or through the use of neurotropic viruses such as Theiler's murine encephalomyelitis virus[1,4,41,42]. In these experimental models, demyelination occurs in multiple regions of the central nervous system in a manner that mimics a specific disease. Since demyelination and remyelination processes can progress simultaneously in these models, it is generally not possible to evaluate demyelination or remyelination in isolation. Another demyelination model involves the use of toxins. The main toxins used are lysophosphatidylcholine, ethidium bromide, and cuprizone. In rodents, cuprizone intake induces demyelination by causing oligodendrocyte death in various brain regions—most notably in white matter tracts such as the corpus callosum, internal capsule, anterior commissure, cerebellar peduncles, and the white matter of the thalamus[13,15]. In cuprizone-induced demyelination, the preservation of blood–brain barrier integrity distinguishes it from experimental autoimmune encephalomyelitis[50]. Another model of toxin-induced demyelination is lysophosphatidylcholine-induced demyelination[14,43]. This membrane disrupting agent was first used by Hall et al.[43]. It is a chemical that induces focal demyelination when stereotactically injected into the white matter tracts of the central nervous system. The main advantage of this model is its ability to be applied locally. Its disadvantage, however, is that the demyelination caused by lysophosphatidylcholine is related to the direct toxic damage to myelin rather than an immune-mediated mechanism.These experimental models can induce demyelination in the central nervous system; however, if the aim is to investigate demyelination caused by the mechanical compression of tumors originating from the sellar/parasellar region on the optic chiasm, an experimental model that mimics the compression effect of the tumor on the optic chiasm becomes prominent. The difference between our experimental model and other models that induce demyelination is that our model creates demyelination directly in the targeted tissue without causing chemical damage. Another difference is that the duration and strength of the compression that causes demyelination can be adjusted. An advantage of using pressure is that once the pressure is removed, all subsequent effects depend on the initial compression. Therefore, the processes of demyelination and remyelination include independent time frames.

Currently, treatments aimed at increasing remyelination generally focus on two major principles, viz., transplantation of exogenous cells and stimulation of endogenous remyelination. In transplantation studies of exogenous cells, transplantations of oligodendrocyte progenitor cells[44], schwann cells[45,46], and embryonic stem cell-derived glial progenitor cells[47] have been performed in demyelinated areas, yielding positive results after transplantation. Nonetheless, some issues must be addressed for exogenous cell transplantation therapies, including the ideal stem cell source, the route of transplantation, the differentiation of the stem cell in the targeted tissue, and its functional and long-term integration. These issues reduce the practical applicability of exogenous cell transplantation and increase its invasiveness. Another method involves studying the efficient functioning of the endogenous regenerative process for remyelination, considering the abundance of oligodendrocyte progenitor cells in the adult central nervous system. For instance, the effects of exogenously intraventricularly administered bone morphogenetic protein on remyelination were investigated in a model of demyelination induced by cuprizone in mice[51]. Our study was planned to induce endogenous remyelination, and we observed that myricetin administration ultrastructurally reduced demyelination and increased remyelination. Compared with the

 doi:10.20944/preprints202507.2316.v1

abovementioned remyelination-improving treatments, myricetin has the advantages of easy access and practically less invasive route of administration (intraperitoneal).

Recent evidence suggests that myricetin exerts a range of neuroprotective effects through multiple cellular mechanisms, including its anti-inflammatory, antioxidant, and anti-apoptotic properties. One of the primary pathways involves the suppression of lipopolysaccharide-induced neuroinflammation, achieved by downregulating pro-inflammatory mediators such as TNF-α and IL-1β, and inhibiting microglial activation[21,52]. Myricetin also modulates oxidative stress by scavenging reactive oxygen species and enhancing endogenous antioxidant defenses, contributing to neuronal survival in preclinical models[31,53]. In addition, it has been shown to directly inhibit apoptotic signaling cascades, including the suppression of caspase-3 activation, thereby protecting neurons from glutamate-induced excitotoxicity[54]. Beyond its molecular effects, myricetin has demonstrated potential therapeutic relevance in a variety of neurological, neuropsychiatric, and neurodegenerative disease models, including Alzheimer's, Parkinson's, and ischemic stroke[55,56]. Its pleiotropic actions have been further supported by recent reviews summarizing its pharmacokinetics, blood–brain barrier permeability, and its role in modulating pathways such as MAPK, PI3K/Akt, and NF-κB[21,23]. These effects of myricetin may provide a plausible biological basis for the ultrastructural improvements observed in our model, particularly regarding the attenuation of axonal degeneration and support for remyelination. In our study, animals treated with myricetin showed a relative reduction in dark degeneration, vacuolization, and demyelination in the optic chiasm compared to untreated animals, as observed through electron microscopy. Although our findings are based on morphological assessment, they appear consistent with previously reported neuroprotective mechanisms of myricetin. Additional studies that include molecular analyses may help to more clearly define the potential role of myricetin in demyelinating conditions, including those related to compressive optic pathway injury.

The present study was aimed to mimic the demyelination caused by the pressure exerted by lesions in the sellar/parasellar region on the optic chiasm; however, it has some limitations. Lesions in the sellar/parasellar region generally grow over a certain period, and the increasing tumor volume during this growth period results in a gradual increase in the pressure exerted on the optic chiasm. Our model more closely resembles the acute compression caused by a sudden increase in volume, such as apoplexy in pituitary adenomas. Therefore, the demyelination-reducing/remyelination-increasing effect of myricetin that we demonstrated in this study affects the demyelination that develops due to the acute pressure on the optic chiasm. However, this experimental model and the positive results of myricetin administration will lead to follow-up studies that will investigate different durations of pressure, various doses of myricetin, or other agents that can stimulate endogenous remyelination.

Another important limitation of our study is the lack of molecular analysis to elucidate the mechanistic pathways through which myricetin exerts its potential remyelinating effects. Our primary aim was to evaluate morphological changes in a pressure-induced demyelination model by electron microscopy. We acknowledge that evaluating molecular signaling cascades such as the Nrf2 antioxidant pathway, PI3K/Akt signaling, and inflammatory mediators would provide a deeper understanding of the biological processes involved.

5. Conclusions

This study serves as another example of experimental models with demyelination induced by compression on the optic chiasm, which is rarely described in the literature. External pressure was applied to the optic chiasm, and demyelination was demonstrated by electron microscopy. Furthermore, we demonstrated the positive effects of myricetin on remyelination after the removal of the compression. This study may provide an opportunity to explore the effects of different agents on demyelination and remyelination in the optic chiasm as an experimental model, and with subsequent studies, it may allow including myricetin treatment protocols for demyelinated nerve cells.

 doi:10.20944/preprints202507.2316.v1

Author Contributions: E.Y. Writing—original draf, sofware, visualization. I.A. Supervision, writing—review and editing, project administration. S.K. Histopathological examination. A.E. Sofware, resources, investigation. A.U. Sofware, resources, investigation. A.K. Physiological research and examination, experimental management. S.B. Statistical analysis evaluation. A.G. formal analysis, data curation. M.Ç. formal analysis, data curation. B.Ç. Supervision, writing—review and editing. S.C. Conceptualizations, methodology, project administration.

Funding: This study was partially supported by Kocaeli University Scientific Research Projects Coordination Unit.

Institutional Review Board Statement: All animal experiments were conducted in accordance with the principles of laboratory animal care. Project No: KOÜ HADYEK 7/1-2022 decision number for this research was approved by Kocaeli University Animal Experiments Local Ethics Committee on 28/12/2022.

Informed Consent Statement: Not applicable.

Data Availability: The data and materials used in the study are in the archives of our hospital.The datasets used and/or analysed during the current study available from the corresponding author on reasonable request.

Conflicts of Interest: The authors declare no conflict of interest.

Acknowledgments: Preparation for publication of this article is partly supported by Turkish Neurosurgical Society.

References

1. Gold, R., Hartung, H. P., & Toyka, K. V. (2000). Animal models for autoimmune demyelinating disorders of the nervous system. Molecular medicine today, 6(2), 88- 91.
2. Osorio-Querejeta, I., Sáenz-Cuesta, M., Muñoz-Culla, M., & Otaegui, D. (2017). Models for studying myelination, demyelination and remyelination. *Neuromolecular medicine*, *19*, 181-192.
3. Tanaka, T., & Yoshida, S. (2014). Mechanisms of remyelination: recent insight from experimental models. *Biomolecular concepts*, *5*(4), 289-298.
4. Torre-Fuentes, L., Moreno-Jiménez, L., Pytel, V., Matías-Guiu, J. A., Gómez-Pinedo, U., & Matías-Guiu, J. (2020). Modelos experimentales de desmielinización-remielinización. *Neurología*, *35*(1), 32-39.
5. Levkovitch-Verbin, H. (2004). Animal models of optic nerve diseases. *Eye*, *18*(11), 1066-1074.
6. Benowitz, L. I., & Yin, Y. (2010). Optic nerve regeneration. *Archives of ophthalmology*, *128*(8), 1059-1064.
7. Torre-Fuentes, L., Moreno-Jiménez, L., Pytel, V., Matías-Guiu, J. A., Gómez-Pinedo, U., & Matías-Guiu, J. (2020). Experimental models of demyelination and remyelination. *Neurología (English Edition)*, *35*(1), 32-39.
8. Li, H. Y., Ruan, Y. W., Ren, C. R., Cui, Q., & So, K. F. (2014). Mechanisms of secondary degeneration after partial optic nerve transection. *Neural regeneration research*, *9*(6), 565-574.
9. Benowitz, L. I., He, Z., & Goldberg, J. L. (2017). Reaching the brain: Advances in optic nerve regeneration. *Experimental neurology*, *287*, 365-373.
10. Sun, W., Chao, G., Shang, M., Wu, Q., Xia, Y., Wei, Q., ... & Liao, L. (2023). Optic nerve injury models under varying forces. *International Ophthalmology*, *43*(3), 757-769.
11. Solomon, A. S., Lavie, V., Hauben, U., Monsonego, A., Yoles, E., & Schwartz, M. (1996). Complete transection of rat optic nerve while sparing the meninges and the vasculature: an experimental model for optic nerve neuropathy and trauma. Journal of neuroscience methods, 70(1), 21-25.
12. Cameron, E. G., Xia, X., Galvao, J., Ashouri, M., Kapiloff, M. S., & Goldberg, J. L. (2020). *Optic nerve crush in mice to study retinal ganglion cell survival and regeneration. Bio-protocol, 10 (6), e3559*.
13. M. Kipp, T. Clarner, J. Dang, S. Copray, and C. Beyer, "The cuprizone animal model: New insights into an old story," Acta Neuropathologica. 2009, doi: 10.1007/s00401- 009-0591-3.
14. J. R. Plemel et al., "Mechanisms of lysophosphatidylcholine-induced demyelination: A primary lipid disrupting myelinopathy," Glia, 2018, doi: 10.1002/glia.23245.
15. Torkildsen, Ø., Brunborg, L. A., Myhr, K. M., & Bø, L. (2008). The cuprizone model for demyelination. *Acta neurologica scandinavica*, *117*, 72-76.
16. Laws, E. R., Trautmann, J. C., & Hollenhorst, R. W. (1977). Transsphenoidal decompression of the optic nerve and chiasm: visual results in 62 patients. Journal of neurosurgery, 46(6), 717-722.

 doi:10.20944/preprints202507.2316.v1

17. Kerrison, J. B., Lynn, M. J., Baer, C. A., Newman, S. A., Biousse, V., & Newman, N. J. (2000). Stages of improvement in visual fields after pituitary tumor resection.American journal of ophthalmology, 130(6), 813-820.
18. Anik, I., Anik, Y., Cabuk, B., Caklili, M., Pirhan, D., Ozturk, O., ... & Ceylan, S. (2018). Visual outcome of an endoscopic endonasal transsphenoidal approach in pituitary macroadenomas: quantitative assessment with diffusion tensor imaging early and long-term results. World Neurosurgery, 112, e691-e701.
19. Anik, I., Anik, Y., Koc, K., Ceylan, S., Genc, H., Altintas, O., ... & Baykal Ceylan, D. (2011). Evaluation of early visual recovery in pituitary macroadenomas after endoscopic endonasal transphenoidal surgery: Quantitative assessment with diffusion tensor imaging (DTI). Acta neurochirurgica, 153(4), 831-842.
20. Emengen, A., Anik, I., Kokturk, S., Karson, A., Yilmaz, E., Basaran, E., ... & Ceylan, S. (2022). Investigation of Demyelination and Remyelination Processes of the Compressed Optic Chiasm: An Experimental Model. *Turkish Neurosurgery*.
21. Song, X., Tan, L., Wang, M., Ren, C., Guo, C., Yang, B., ... & Pei, J. (2021). Myricetin: A review of the most recent research. *Biomedicine & Pharmacotherapy*, *134*, 111017.
22. Hou, W., Hu, S., Su, Z., Wang, Q., Meng, G., Guo, T., ... & Gao, P. (2018). Myricetin attenuates LPS-induced inflammation in RAW 264.7 macrophages and mouse models. *Future medicinal chemistry*, *10*(19), 2253-2264.
23. Jiang, M., Zhu, M., Wang, L., & Yu, S. (2019). Anti-tumor effects and associated molecular mechanisms of myricetin. *Biomedicine & Pharmacotherapy*, *120*, 109506.
24. Stoll, S., Bitencourt, S., Laufer, S., & Inês Goettert, M. (2019). Myricetin inhibits panel of kinases implicated in tumorigenesis. *Basic & Clinical Pharmacology & Toxicology*, *125*(1), 3-7.
25. Jiang, S., Tang, X., Chen, M., He, J., Su, S., Liu, L., ... & Xue, W. (2020). Design, synthesis and antibacterial activities against Xanthomonas oryzae pv. oryzae, Xanthomonas axonopodis pv. Citri and Ralstonia solanacearum of novel myricetin derivatives containing sulfonamide moiety. *Pest management science*, *76*(3), 853-860.
26. Ortega, J. T., Suárez, A. I., Serrano, M. L., Baptista, J., Pujol, F. H., & Rangel, H. R. (2017). The role of the glycosyl moiety of myricetin derivatives in anti-HIV-1 activity in vitro. *AIDS research and therapy*, *14*, 1-6.
27. Wang, L., Wu, H., Yang, F., & Dong, W. (2019). The protective effects of myricetin against cardiovascular disease. *Journal of nutritional science and vitaminology*, *65*(6), 470-476.
28. Guo, C., Xue, G., Pan, B., Zhao, M., Chen, S., Gao, J., ... & Qiu, L. (2019). Myricetin ameliorates ethanol-induced lipid accumulation in liver cells by reducing fatty acid biosynthesis. *Molecular nutrition & food research*, *63*(14), 1801393.
29. Ahmed, S., Khan, H., Aschner, M., Hasan, M. M., & Hassan, S. T. (2019). Therapeutic potential of naringin in neurological disorders. *Food and chemical toxicology*, *132*, 110646.
30. Wang, Q. M., Wang, G. L., & Ma, Z. G. (2016). Protective effects of myricetin on chronic stress-induced cognitive deficits. *Neuroreport*, *27*(9), 652-658.
31. Li, J., Xiang, H., Huang, C., & Lu, J. (2021). Pharmacological actions of myricetin in the nervous system: a comprehensive review of preclinical studies in animals and cell models. *Frontiers in Pharmacology*, *12*, 797298.
32. Zhang, Q., Li, Z., Wu, S., Li, X., Sang, Y., Li, J., ... & Ding, H. (2016). Myricetin alleviates cuprizone-induced behavioral dysfunction and demyelination in mice by Nrf2 pathway
33. Wang, B., Zhong, Y., Gao, C., & Li, J. (2017). Myricetin ameliorates scopolamine-induced memory impairment in mice via inhibiting acetylcholinesterase and down-regulating brain iron. *Biochemical and biophysical research communications*, *490*(2), 336-342.
34. Meyer, E., Mori, M. A., Campos, A. C., Andreatini, R., Guimarães, F. S., Milani, H., & de Oliveira, R. M. W. (2017). Myricitrin induces antidepressant-like effects and facilitates adult neurogenesis in mice. *Behavioural Brain Research*, *316*, 59-65.
35. Kim, H. D., Jeong, K. H., Jung, U. J., & Kim, S. R. (2016). Myricitrin ameliorates 6-hydroxydopamine-induced dopaminergic neuronal loss in the substantia nigra of mouse brain. *Journal of medicinal food*, *19*(4), 374-382.

 doi:10.20944/preprints202507.2316.v1

36. Wu, S., Yue, Y., Peng, A., Zhang, L., Xiang, J., Cao, X., ... & Yin, S. (2016). Myricetin ameliorates brain injury and neurological deficits via Nrf2 activation after experimental stroke in middle-aged rats. *Food & function*, *7*(6), 2624-2634.
37. Paxinos, G., & Watson, C. (2006). *The rat brain in stereotaxic coordinates: hard cover edition*. Elsevier.
38. Clifford-Jones, R. E., Landon, D. N., & McDonald, W. I. (1980). Remyelination during optic nerve compression. Journal of the neurological sciences, 46(2), 239-243.
39. Giacci, M. K., Bartlett, C. A., Huynh, M., Kilburn, M. R., Dunlop, S. A., & Fitzgerald, M. (2018). Three dimensional electron microscopy reveals changing axonal and myelin morphology along normal and partially injured optic nerves. Scientific reports,8(1), 1-12.
40. Xie, F., Liang, P., Fu, H., Zhang, J. C., & Chen, J. (2014). Effects of normal aging on myelin sheath ultrastructures in the somatic sensorimotor system of rats. *Molecular Medicine Reports*, *10*(1), 459-466.
41. Denic, A., Johnson, A. J., Bieber, A. J., Warrington, A. E., Rodriguez, M., & Pirko, I. (2011). The relevance of animal models in multiple sclerosis research.Pathophysiology, 18(1), 21-29.
42. Dal Canto, M. C., Kim, B. S., Miller, S. D., & Melvold, R. W. (1996). Theiler's murine encephalomyelitis virus (TMEV)-induced demyelination: a model for humanmultiple sclerosis. *Methods*, *10*(3), 453-461.
43. HALL, S. M. (1972). The effect of injections of lysophosphatidyl choline into white matter of the adult mouse spinal cord. *Journal of cell science*, *10*(2), 535-546.
44. Windrem, M. S., Nunes, M. C., Rashbaum, W. K., Schwartz, T. H., Goodman, R. A., McKhann, G., ... & Goldman, S. A. (2004). Fetal and adult human oligodendrocyte progenitor cell isolates myelinate the congenitally dysmyelinated brain. *Nature medicine*, *10*(1), 93-97.
45. Bachelin, C., Lachapelle, F., Girard, C., Moissonnier, P., Serguera-Lagache, C., Mallet, J., ... & Baron-Van Evercooren, A. (2005). Efficient myelin repair in the macaque spinal cord by autologous grafts of Schwann cells. *Brain*, *128*(3), 540-549.
46. Franklin, R. J. M., Gilson, J. M., Franceschini, I. A., & Barnett, S. C. (1996). Schwann cell-like myelination following transplantation of an olfactory bulb-ensheathing cell line into areas of demyelination in the adult CNS. *Glia*, *17*(3), 217-224.
47. Brüstle, O., Jones, K. N., Learish, R. D., Karram, K., Choudhary, K., Wiestler, O. D., ... & McKay, R. D. (1999). Embryonic stem cell-derived glial precursors: a source of myelinating transplants. *Science*, *285*(5428), 754-756.
48. Cottee, L. J., Daniel, C., Loh, W. S., Harrison, B. M., & Burke, W. (2003). Remyelination and recovery of conduction in cat optic nerve after demyelination by pressure. *Experimental neurology*, *184*(2), 865-877.
49. Burke, W., Dreher, B., Michalski, A., Cleland, B. G., & Rowe, M. H. (1992). Effects of selective pressure block of Y-type optic nerve fibers on the receptive-field properties of neurons in the striate cortex of the cat. *Visual Neuroscience*, *9*(1), 47-64.
50. Tanaka, T., & Yoshida, S. (2014). Mechanisms of remyelination: recent insight from experimental models. *Biomolecular concepts*, *5*(4), 289-298.
51. Sabo, J. K., Aumann, T. D., Merlo, D., Kilpatrick, T. J., & Cate, H. S. (2011). Remyelination is altered by bone morphogenic protein signaling in demyelinated lesions. *Journal of Neuroscience*, *31*(12), 4504-4510.
52. Jang, J. H., Lee, S. H., Jung, K., Yoo, H., & Park, G. (2020). Inhibitory effects of myricetin on lipopolysaccharide-induced neuroinflammation. *Brain Sciences, 10*(1), 32.
53. Bellavite, P. (2023). Neuroprotective potentials of flavonoids: Experimental studies and mechanisms of action. *Antioxidants*, *12*(2), 280.
54. Shimmyo, Y., Kihara, T., Akaike, A., Niidome, T., & Sugimoto, H. (2008). Three distinct neuroprotective functions of myricetin against glutamate-induced neuronal cell death: involvement of direct inhibition of caspase-3. *Journal of neuroscience research*, *86*(8), 1836-1845.
55. Sethiya, N. K., Ghiloria, N., Srivastav, A., Bisht, D., Chaudhary, S. K., Walia, V., & Alam, M. S. (2024). Therapeutic potential of myricetin in the treatment of neurological, neuropsychiatric, and neurodegenerative disorders. *CNS & Neurological Disorders - Drug Targets, 23*(7), 865–882.
56. Aoi, W., Iwasa, M., & Marunaka, Y. (2021). Metabolic functions of flavonoids: From human epidemiology to molecular mechanism. *Neuropeptides, 88*, 102163.

 doi:10.20944/preprints202507.2316.v1